J. Membrane Biol. 14, 383–402 (1973)

The Ultrastructural Localization and Quantitation of Cholinergic Receptors at the Mouse Motor Endplate

C. W. Porter, E. A. Barnard * and T. H. Chiu

Departments of Pathology, Biochemistry and Biochemical Pharmacology, State University of New York, Buffalo, New York 14214

Received 15 January 1973; revised 19 September 1973

Summary. The snake venom toxin, α-bungarotoxin, is known to bind specifically to the acetylcholine receptor at skeletal muscle endplates. In this study, tritiated α-bungarotoxin has been used in conjunction with electron-microscope autoradiography to visualize and enumerate acetylcholine receptor sites at the neuromuscular junctions of the mouse diaphragm. From an analysis of the grain distribution, the receptor sites appear to be located specifically on the postjunctional membrane. The density there is about 8,500/μ^2 of membrane surface. For comparison purposes, cholinesterases and related active centers were labeled using [^{3}H] diisopropylfluorophosphate; they were shown to be at this same concentration over the synaptic membranes (or along the cleft). The 1:1 relationship of the receptors to the cholinesterase type of site, found previously to hold in studies on whole endplates, is also true at the ultrastructural level in this case. In fact, this 1:1 relationship is believed to be a characteristic of the postsynaptic membranes of endplates in other muscles and other vertebrates.

Based on the constant density value thus arrived at, the total surface areas of postsynaptic and of presynaptic membranes are at once obtained from the known total numbers of these sites per endplate, available from previous studies in this laboratory. Examples of such synaptic surface area values are given. These values are only reliable for a given muscle type if the approximate fiber size is defined.

By use of the labeled inhibitor autoradiographic method (Barnard, 1970), the absolute numbers of acetylcholinesterase (AChE) active sites at individual motor endplates have been determined in a number of vertebrate muscle types (Rogers, Darzynkiewicz, Salpeter, Ostrowski & Barnard, 1969; Barnard, Rymaszewska & Wieckowski, 1971*a*). The inhibitor used was ^{3}H- or ^{32}P-labeled diisopropylfluorophosphate (DFP). Specificity for the active centers of AChE was obtained by the parallel application of the specific reactivator (Wilson, Ginsburg & Quan, 1958), pyridine-2-aldoxime methiodide (2-PAM), as well as by the protection from the DFP reaction exerted by selective, reversible inhibitors of AChE. It was shown thus that in endplates of mouse and rat striated muscles, one-third of the total sites readily

* Correspondence and reprint requests should be addressed to this author, at the Department of Biochemistry.

reactive towards DFP are AChE active centers (Rogers *et al.*, 1969; Barnard *et al.*, 1971*a*).

These methods can be extended to the ultrastructural level, by using electron-microscope (EM) autoradiography [for a review, *see* Budd (1971)]. The ^{3}H-DFP reaction has been applied thus (Rogers, Darzynkiewicz, Barnard & Salpeter, 1966; Salpeter, 1967, 1969), with results showing that there are about 9,000 DFP-reactive sites per μ^2 of junctional membrane at the mouse motor endplates studied (Salpeter, Plattner & Rogers, 1972). One-third of these, again, appear to be AChE active centers. The results so far obtained support the asssumption that there is a constant density of AChE molecules in or associated with the postsynaptic membranes (Salpeter *et al.*, 1972; Barnard, 1974).

It is of importance to discover whether this constant surface density holds true also for the acetylcholine (ACh) receptor molecules at the synapse. Barnard, Wieckowski and Chiu (1971*b*) have shown that light microscope autoradiography can be utilized to count the number of these receptors per junction, by exploiting the great specificity and irreversibility of their reaction with α-bungarotoxin (α-BuTX). This snake venom toxin was labeled with tritium by a ^{3}H-acetylation reaction that leaves its neurotoxic properties quantitatively unimpaired (Barnard *et al.*, 1971*b*; Albuquerque, Barnard, Chiu, Lapa, Dolly, Jaenssen, Daly & Witkop, 1973; Porter, Chiu, Wieckowski & Barnard, 1973). The availability of this fully active ^{3}H-α-BuTX, and its application in the EM autoradiographic technique, permit, as was indicated in a preliminary report (Porter *et al.*, 1973), the absolute measurement of ACh receptor sites in relation to endplate ultrastructure. We report here more detailed studies that yield the density at the postsynaptic membrane.

Materials and Methods

Materials

Pure α-BuTX was prepared and labeled by ^{3}H-acetylation as described elsewhere (Barnard *et al.*, 1971*b*). The preparation (used at specific activities of 4.1 or 6.65 C/mmole) showed no change in toxicity as measured by survival time of mice injected intravenously (1.5 μg/g) or blockade of phrenic nerve–diaphragm preparations *in vitro* (Barnard *et al.*, 1971*b*). ^{3}H-DFP (3.6 C/mmole) was obtained from Amersham Searle Co., Illinois and handled as described by Rogers *et al.* (1969). Rockefeller (RR) strain albino male mice weighing 20 to 25 g were used in all experiments.

^{3}H-α-Bungarotoxin Labeling and Analysis

Labeling. Mice were injected via the tail vein with a supra-lethal dose (1.5 μg/g body weight) of ^{3}H-α-BuTX. Immediately after death, usually about 4 min after injection,

the diaphragm was removed, rinsed in 0.1 M phosphate buffer (pH 7.4), and fixed in 3% glutaraldehyde in the same buffer for 2 hr at 4 °C. Endplate-rich areas of the diaphragm were then dissected out, postfixed in 1% osmium tetroxide, dehydrated in graded alcohols, and embedded in Epon-Araldite. In later work, 0.2 M sucrose was in the buffers.

Autoradiography. The autoradiographic methods of Salpeter and Bachman (1964) were used. The ultramicrotome sections were selected to be about 1,000 Å thick by their pale gold interference color. Their thickness was checked by precise measurement on samples, and gave a mean of 993 Å (SD 92 Å) thickness. These latter measurements were made at 2,946 Å wavelength on an Angstrom-scope interferometer (Varian Instruments, Palo Alto, California). The sections were mounted on collodionized slides, stained with 2% uranyl acetate, carbon coated and overlaid with a monolayer of Ilford L-4 emulsion. They were exposed 30 to 60 days for toxin-labeled muscle and 57 days for DFP-labeled muscle. Exposed slides were developed with Microdol X (Eastman Kodak Co., Rochester, N.Y.), 2 min at room temperature.

Analysis of Autoradiographs. Sections were mounted on 100-mesh grids and examined with the electron-microscope (Siemens Elmiskope 101). All endplates encountered, regardless of grain concentration, were photographed so that the final magnification was 30,000 ×. At times, several photographs were required to include the entire endplate and surrounding tissue to a depth of at least 2 μ. Photographs were taken at random for background computations. Area determinations were made by overlaying a plastic transparency containing a uniform lattice-point grid (1 point $\equiv 0.25\ \mu^2$ at 30,000 ×) and counting the number of points that fell over each tissue compartment.

Identification of the Sites of Bound Isotope. Histograms were prepared by measuring the distance of each geometric grain center or grid point to the nearest suspected source of radioactivity—in this case, the axonal or postjunctional membrane. The distances were tabulated in columns of 1,600 Å on either side of the given membrane. In distribution histograms, distances on the axon side of the membrane were given a negative sign and those on the muscle side a positive sign. The grain count for each such column was divided by the corresponding set of random points to obtain a density in grains/μ^2, which refers to uniformly standardized areas throughout. The distances were expressed in units of half distance (HD)[1]. Finally, the grain density was "normalized" by setting the grain count for the column containing the suspected line source (HD = 0) equal to unity, and adjusting the values for the other columns proportionally.

Quantitative Analysis. Molecular estimates are made on the basis that one radioactive toxin molecule binds irreversibly to one enzyme or receptor active site, respectively. Knowing the specific activity of the labeled reagent, the exposure time, and the sensitivity of the autoradiographic system, one can determine by a simple calculation the number of molecules represented by one grain [*see* Salpeter *et al.* (1972) for details]. Lengths of membrane profiles present were determined with a map measurer. Grain values related to structural components were multiplied by 10 to correspond to a section one micron in thickness.

The sensitivity of the autoradiographic system is one of the values necessary for this quantitative estimation. Sensitivity is the number of radioactive decays required to produce one grain. Salpeter and Szabo (1972) have found that the sensitivity is related to radiation dose and thus to grain density over the labeled area. In the case of labeled endplates, the cleft substance which separates the axonal and postjunctional membranes has been used (Salpeter *et al.*, 1972; Salpeter & Szabo, 1972) as a logical indicator of

1 HD is an experimental measure of resolution for a given autoradiographic system; it indicates the distance from a radioactive line source within which 50% of the developed grains fall. For further details, *see* Salpeter *et al.* (1969). In this study, 1 HD = 1,600 Å.

radiation dose. The molecular calculations used here are based on a sensitivity value of 1 grain per 10.7 radioactive decays, determined by Dr. G. C. Budd (Toledo, Ohio) for our L-4 emulsion batch (Batch 26558) at a radiation dose level of 0.5 grains/μ^2. Since the experimental grain density per μ^2 of cleft substance was 0.46 in this study, the sensitivity value is directly applicable without reference to the dose dependence curve of Salpeter and Szabo (1972). In determining the densities of labeled sites per unit surface area of membrane, the histogram centered on the postjunctional membrane (*see* Results) was used. All of the grains that contributed to it in the area within the theoretical distribution curve (Salpeter, Bachmann & Salpeter, 1969) for a line source at that membrane were considered, and their numbers converted to molecular sites relative to the area of membrane involved. Since the resolution limit of L-4 emulsion does not permit us to distinguish between radioactivity at presynaptic and postsynaptic sites where these are opposed at the primary cleft, this total of grains was, alternatively, related to the sum of presynaptic and postsynaptic areas involved. The membrane surface areas cited assume a vertical orientation of the membrane in relation to the plane of the section, so that the true density is likely to be somewhat below the densities calculated here for this ideal case.

The density of label over the muscle sarcolemma was also determined, for comparison. Non-endplate-associated sarcolemma in the same sections was measured with a map measurer and all grains within 3,000 Å were considered membrane-related, to allow for radiation scatter (Salpeter, 1967). The grain density was converted to sites/μ^2 as above.

Comparison of ^{3}H-α-BuTX and ^{3}H-DFP Binding

^{3}H-DFP Labeling. Mice were killed by cervical disjunction. Small blocks of diaphragm were dissected out and fixed in 3% buffered glutaraldehyde for 1 hr at 4 °C. [Such fixation does not reduce ^{3}H-DFP uptake (Rogers *et al.*, 1969).] The muscle was then washed in buffer and incubated in 1×10^{-4} M ^{3}H-DFP in 0.067 M phosphate buffer (pH 7.4) for 30 min. After several buffer washes, the muscle was placed in nonradioactive DFP (1×10^{-3} M) for 20 min to exchange with ^{3}H-DFP bound nonspecifically. The labeled tissue was post-fixed in OsO_4 and embedded as above.

Autoradiography and Analysis. In a separate experiment, ^{3}H-DFP and ^{3}H-α-BuTX labeled tissues were prepared and processed for EM autoradiography by the procedures noted above. Coated tissue was exposed for time periods inversely proportional to the specific activity of the label preparation, so that, if equal numbers of the two types of binding site were present, each ^{3}H-DFP- or ^{3}H-α-BuTX-labeled endplate would experience the same number of radioactive decays. That is, the exposure time was adjusted such that the product of the exposure time in days and the specific activity of the label was equal for both preparations (Table 2). In this way, grain counts obtained from autoradiograms of ^{3}H-DFP- or ^{3}H-α-BuTX-labeled endplates could be compared directly. DFP binding at mouse diaphragm endplates has already been thoroughly studied by Salpeter *et al.* (1972). Since that meticulous study is available, and we used the same muscle type, a full analysis of the DFP binding was not necessary here, and a simpler relative method was adequate for our purpose. Since the grain density over endplates labeled with either ^{3}H-DFP or ^{3}H-α-BuTX is known (Salpeter *et al.*, 1972) to agree closely with theoretical curves for a source centered on the postjunctional membrane, it is reasonable to compare grain counts at endplates in relation to membrane lengths without preparing histograms of grain density distributions. Therefore, developed endplates were photographed in a similar manner for both labeling treatments. Total postjunctional membrane lengths and counts of grains associated with the subneural apparatus of each of the endplate profiles were summed separately for

^{3}H-DFP-treated and ^{3}H-α-BuTX-treated endplates. The ratio of grains to membrane lengths was then compared, to test the 1:1 enzyme-to-receptor relationship discerned by other techniques (Barnard *et al.*, 1971*b*) for whole endplates.

Results

A. ACh Receptors at the Mouse Endplate

After a lethal injection of ^{3}H-α-BuTX, followed by processing of the muscle for EM autoradiography, the endplates in the mouse diaphragm were well labeled, with little grain density over the muscle (Table 1). Apart from the endplates, only blood vessel lumens and large bundles of collagen showed significant radioactivity. That quantitative uptake of ^{3}H-α-BuTX occurs at the endplates to a level of saturation, in the labeling conditions used in this study, has already been documented by the use of other techniques (Barnard *et al.*, 1971*b*; Porter *et al.*, 1973).

While all the endplates encountered were photographed, an attempt was made to use, in the grain distribution analysis, those in which the plane of sectioning was nearly perpendicular to the axon and folds and which displayed typical endplate architecture. Fig. 1*A* shows a representative

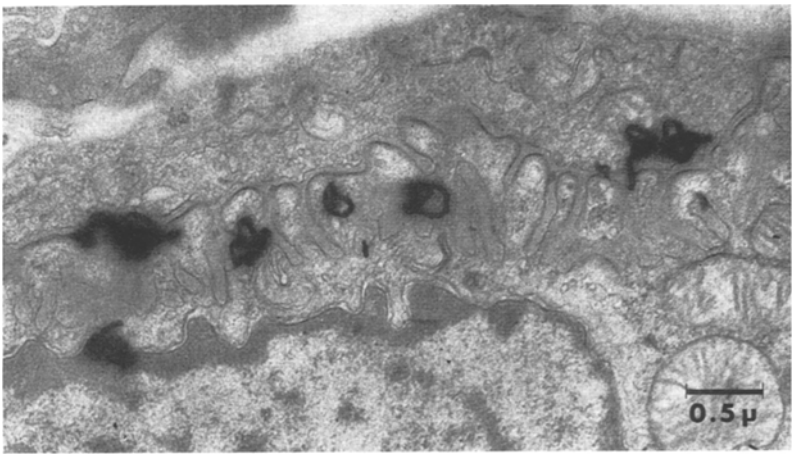

Fig. 1*A*

Fig. 1. (*A*) Autoradiograph of a portion of an endplate labeled with ^{3}H-α-bungarotoxin. Typically, the grains are distributed over the postjunctional folds or within the range of radiation scatter. (× 34,000). (*B*) A portion of an endplate after labeling with ^{3}H-DFP. The axon (*A*) is embedded in a trough in the muscle and surrounded by elaborate folds of postjunctional membrane (*PJF*). Within the axon are a few swollen mitochondria and numerous vesicles presumably containing acetylcholine. Amorphous cleft substance fills the cleft (arrow) between the axon and the muscle fiber and within the folds. The myelinated nerve (*N*) shows no labeling. (× 25,000)

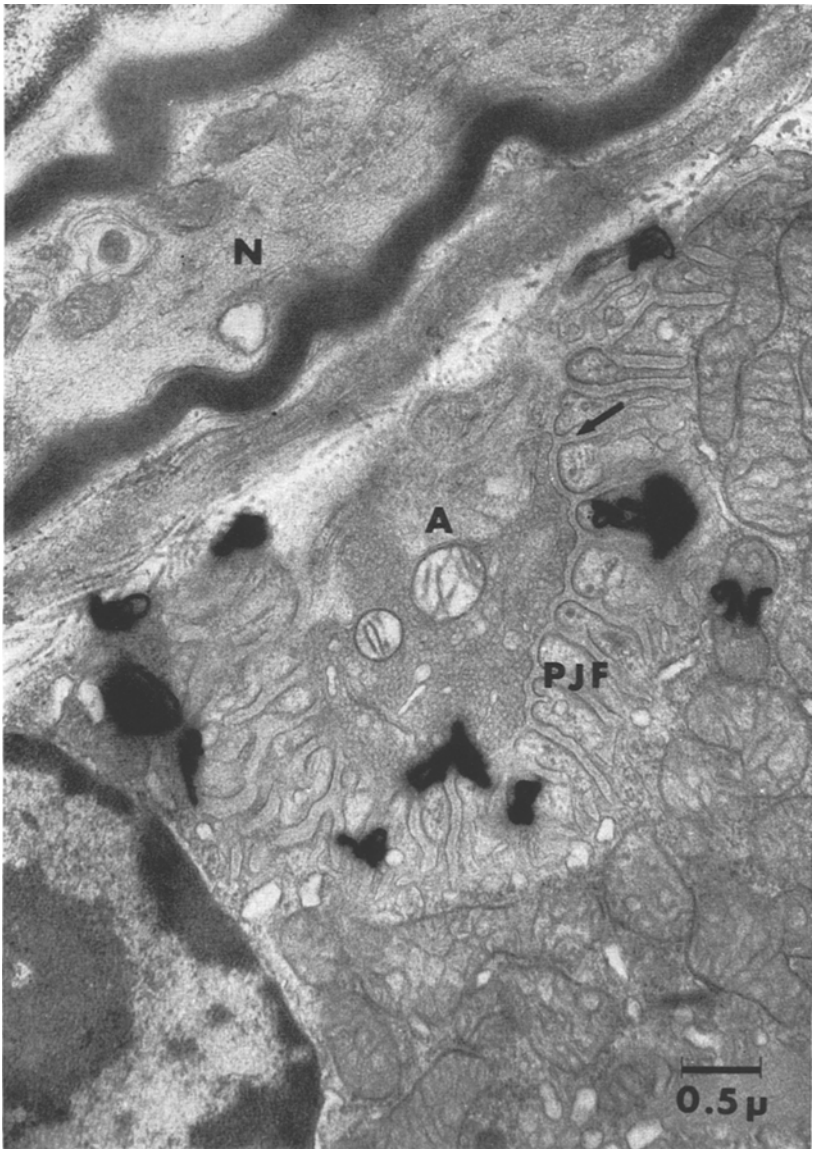

Fig. 1*B*

autoradiogram of a mouse diaphragm endplate labeled with ^{3}H-α-BuTX. On the average, each endplate profile contained about 3 grains, at a density very much higher than that of muscle background. To obtain the grain population used in Figs. 2 and 3, it was necessary to analyze over 100 endplate autoradiograms.

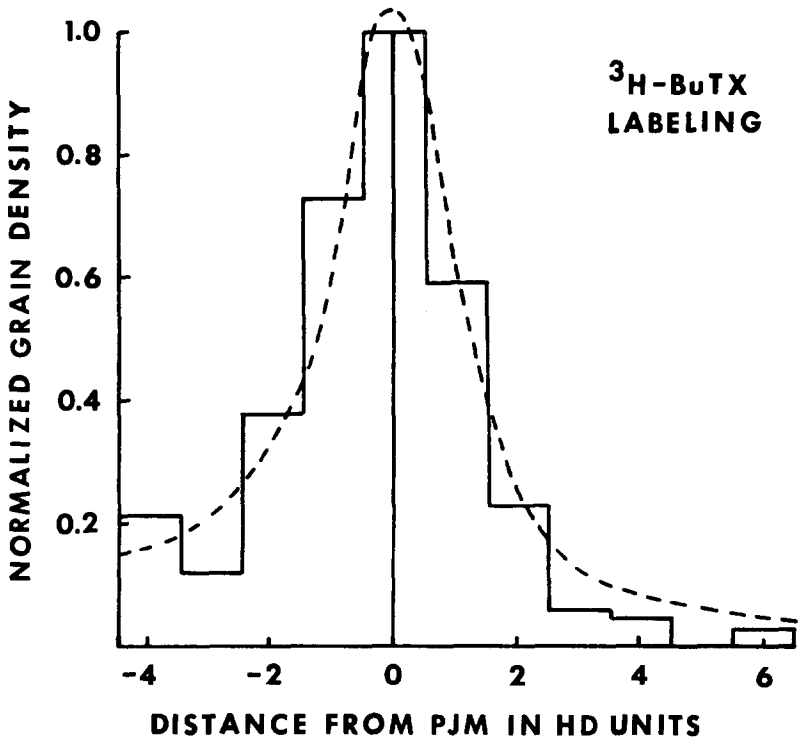

Fig. 2. Histogram showing the experimental grain density distributions around the *postjunctional membrane* (*PJM*) of endplates labeled with ^{3}H-α-bungarotoxin (based on 347 grains and 3,400 points). There is good agreement with a theoretical curve [constructed as described by Salpeter *et al.* (1969)] drawn here for a line source located on the postjunctional membrane and adjusted on the axonal side for the average slight curvature of the end-bulb. In this and the succeeding histograms, the muscle side of the axonal membrane is designated in positive HD units and the axon side in negative units, and the grain density is normalized to 1.0 at the bin containing the line source

In the albino mouse diaphragm, the overwhelming majority of the muscle fibers are of a small diameter (~24 μ) and "red" in type as classified by several standard criteria (Gauthier & Padykula, 1966; Padykula & Gauthier, 1970). The axon is embedded in a trough in the muscle and surrounded by elaborate folds of postjunctional membrane (Fig. 1*B*). Measurements of the lengths of the membranes in our micrographs indicated a ratio of 1:4.5 for axonal and postjunctional membranes, respectively. Within the axon are typically a few mitochondria and many synaptic vesicles. The synaptic space is filled with amorphous cleft substance which extends into the secondary folds and is continuous with the basement membrane. Numerous muscle mitochondria surround the endplate as is typical of red muscle fibers. However, occasional endplates were encoun-

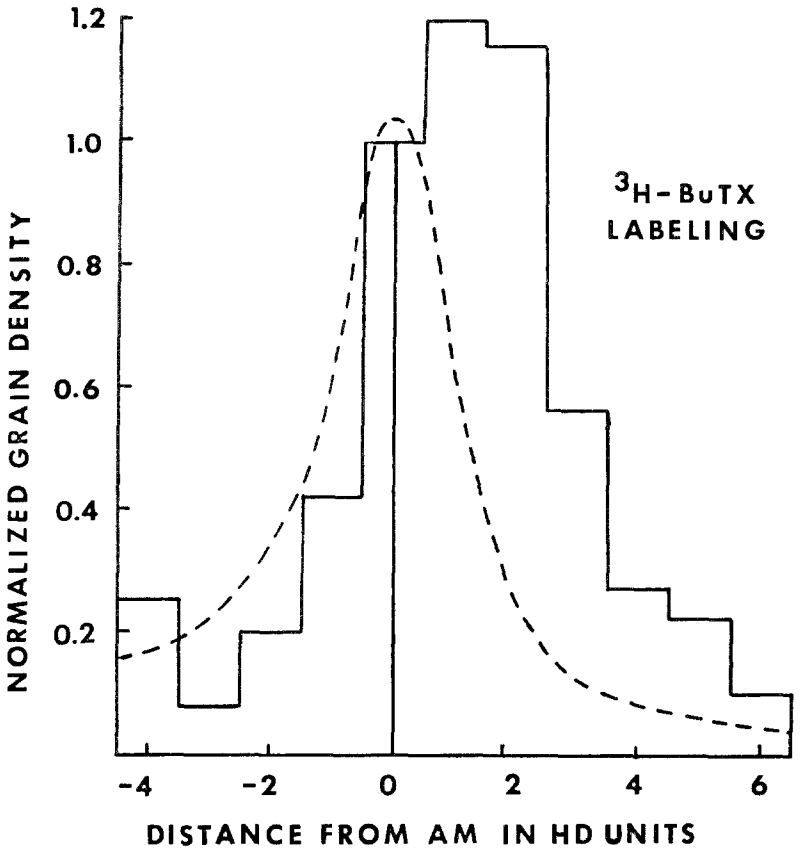

Fig. 3. Experimental grain density distributions around the *axonal membrane* for end-plates labeled with ^{3}H-α-bungarotoxin (based on 333 grains and 2,500 points). The histogram shows no correlation with the theoretical curve drawn, as before, for a line source located on the axonal membrane. Instead, the radiation is shifted to the muscle side (positive HD units) of the axonal membrane over the region of the postjunctional folds

tered on fibers that appeared of the "intermediate" type in the classification noted. These were labeled similarly to the others.

No morphological changes attributable to the toxin action were observed in the interval (less than 10 min) between injection and death. The swollen mitochondria initially observed within the axon were found to be an artifact, and later were eliminated by increasing the tonicity of the fixative.

Identification of Binding Sites. While the bulk of the grains observed were located over the area of the junctional folds, it was still necessary to construct histograms of their location in relation to either the axonal or postjunctional membranes to confirm this distribution for a large number of

endplate profiles. When grain densities are plotted in distances from the postjunctional membrane, the resulting histogram (Fig. 2) closely approximates the theoretical grains curve (Salpeter *et al.*, 1969) of a line source centered on that membrane and adjusted for the average slight curvature of the axon bulb. When plotted, in contrast, in relation to the axonal membrane (Fig. 3), the radioactivity is obviously shifted from under the theoretical curve to the muscle side of the axonal membrane. This corresponds with the region of postjunctional membrane folds. The results of both histograms are most easily compatible with the postjunctional membrane being the site at the endplate of the ACh receptors, although it is not possible in this experiment to exclude a location in the cleft substance. The comparison of Figs. 2 and 3 excludes the case that the bulk of the receptors are located presynaptically, but the possibility remains, at the accessible resolution, of a smaller *additional* number of sites on the axonal membrane.

When the plots from the axonal membrane are confined to grid points and grains lying *only* over junctional folds or membranes (Fig. 4), it is seen that, especially for data in the first four bin columns, the binding over the area of the folds is rather uniform. These first four columns correspond to the average fold depth and represent 75% of the points and 90% of the grains in the total histogram. The grains and points contributing to the last three bin columns are a result of section planes traveling obliquely through some of the folds. In view of the small fractions of the points and the grains represented in this latter area, there must be a lower statistical accuracy there. Therefore, when considered over the area of average folding, the receptor density is, in the limits of the present technique, distributed uniformly from the tips to the depths of the postjunctional folds. In contrast, the treatment used as the basis for Fig. 3 deliberately included, for every HD interval measured from the axonal membrane, an entire zone on the muscle side, whether or not folds were visible there. Variations in the plane of sectioning give an uneven distribution of the folds in the various fields, and as a result, Fig. 3 might mistakenly be interpreted as showing that the receptors are located only at the tips of the folds and decrease in density toward the depths of the folds. When corrected by a plot such as that of Fig. 4, this possibility is tested and removed. The geometry of the folds does not affect the other deductions.

Absolute Quantitation of α-BuTX Binding Sites. The absolute densities of the labeled sites were measured per unit surface area of adjacent membrane. As shown above, the postjunctional membrane is the most likely single source of radioactivity. To make maximum allowance for the resolution

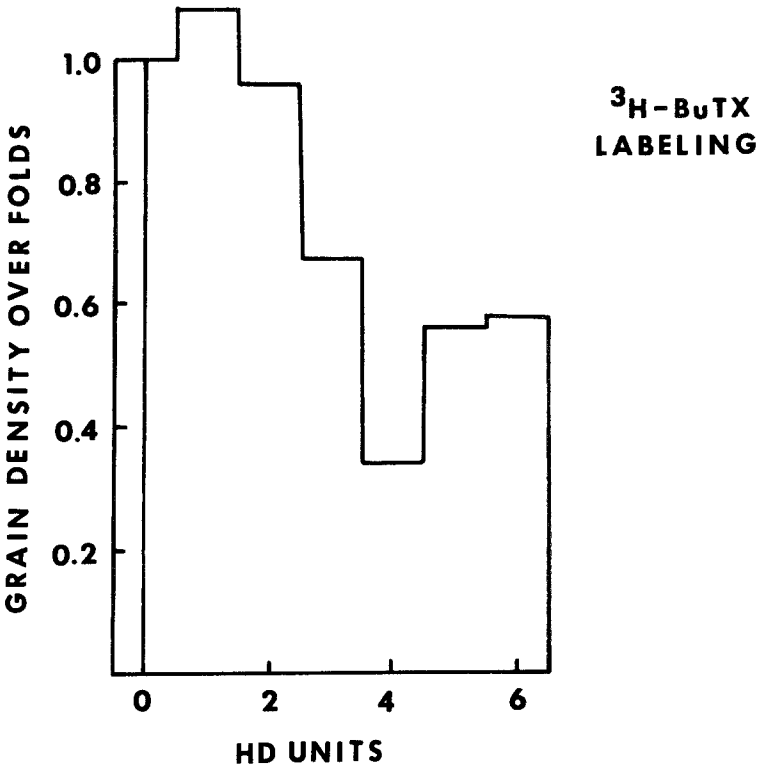

Fig. 4. Histogram of grain densities over the postjunctional folds, as plotted from the *axonal membrane* (based on 283 grains and 1,000 points). Unlike the previous histograms (Figs. 2 and 3), only points and grains that lay actually over the postjunctional folds were considered in determining the grain densities. Note that the areas under this histogram are not a guide to the numbers of counts contributing to the density in the regions in question. In fact, the average fold depth is 0.5 μ, which falls within the first four bin columns; these represent, thus, 90% of the total grains and 75% of the total points used in this histogram, and the last three bins should be given little weight in assessing the distribution here

limitation ($\sim$1,600 Å) in the quantitative analysis all grains lying within the expected distribution curve for a line source centered on the postjunctional membrane were related separately to the postjunctional membrane, postjunctional plus axonal membranes, or cleft substance.

The density of α-BuTX-binding sites found at these sites is presented in Table 1. The number of ACh receptor sites when related solely to the postjunctional membrane is $\sim$8,000 sites/μ^2. If the extreme case is taken of diluting the grain density to include also the entire area of the presynaptic membrane present, and not just that part of it where labeling would be unresolved from postjunctional membrane labeling, then the density in the

Table 1. Densities (per unit area or per unit volume) of binding sites at mouse diaphragm endplates

Structure considered	Binding sites	
	^{3}H-BuTX	^{3}H-DFP [a]
Postjunctional membrane	8,200/μ^2	8,600/μ^2
Postjunctional plus axonal membranes	6,700/μ^2	7,200/μ^2
Cleft substance [b]	141,000/μ^3	130,000/μ^3
Sarcolemma	180/μ^2	
Muscle	430/μ^3	600/μ^3

[a] These values are included here for comparison purposes, from Salpeter *et al.* (1972).
[b] The entire synaptic cleft was taken as the basis.

combined membranes would still be of the same order, ~6,700 sites/μ^2. Finally, when related to the cleft substance volume, the value is 141,000/μ^3.

The density of α-BuTX-binding sites on the muscle cell membrane outside the endplate or within the muscle cell was smaller (Table 1) and clearly did not interfere with the measurements at endplates. Table 1 shows that the increased radioactivity seen in autoradiographs of endplates is not attributable simply to the increase in surface area of the muscle cell membrane that occurs with folding at the nerve junction, but to a specific concentration of binding sites at that junction.

B. Comparison of ^{3}H-DFP and ^{3}H-α-BuTX Binding

The results reported in Section A for α-BuTX binding at the endplate in fact agree closely with those of Salpeter *et al.* (1972) for the uptake of labeled DFP (Table 1). However, absolute EM autoradiography is not such a widely standardized technique that we can exclude the possibility that procedural differences between laboratories could lead to a fortuitous agreement, when different treatments of different animal stocks are made by slightly differing methods in two laboratories. It seemed desirable that we make, also, a direct determination of the ratio noted, with all variables except the reagent kept constant.

Diaphragms labeled with ^{3}H-α-BuTX or with ^{3}H-DFP to saturation of the endplate sites were processed in parallel. By adjusting the exposure times so as to compensate for the specific activities of the ^{3}H-DFP and ^{3}H-α-BuTX reagents available, the grain counts produced in the two types of treated material in relation to known lengths of postjunctional membrane, were made directly comparable in value (Table 2). Salpeter and Szabo

Table 2. Derivation of the 1:1 binding site ratio for active centers of receptors and of ChE-like molecules at the endplate postsynaptic zone

Parameter	Label		
	^{3}H-α-BuTX		^{3}H-DFP
Specific activity (S)	6.7 C/mmole		3.6 C/mmole
Exposure time (t)	30 days		57 days
$S \cdot t$	205		201
Ratio $\frac{S \cdot t \text{ (for BuTX)}}{S \cdot t \text{ (for DFP)}}$		1.01	
Postsynaptically related grains	168 grains		302 grains
Postjunctional membrane length	970 μ		1,700 μ
Grains per μ of postjunctional membrane	0.172		0.177
Ratio of BuTX to DFP sites [a]		0.97	

[a] Expressed as active centers per μ^2 of postjunctional membrane reacting to saturation with the reagent, in each case.

(1972) have shown that proportionality of grain yield to exposure time exists for the emulsion and processing that we employ. For these reasons, we take the comparison of the numbers of grains for known sample lengths of postjunctional membrane to give a valid measure of the density ratio of the two types of binding sites in question; in fact, this appears to be the most accurate method available to us for this purpose. A close agreement was found between grains per μ^2 of membrane for α-BuTX sites and those for DFP sites (Table 2). This confirms that the 1:1 enzyme-to-receptor relationship reported for whole endplates (Barnard *et al.*, 1971*b*) is also true at the ultrastructural level.

Discussion

For reasons cited previously (Barnard *et al.*, 1971*b*; Porter *et al.*, 1973) based upon the known pharmacological and binding properties of α-BuTX, we attribute the uptake of ^{3}H-α-BuTX in the conditions used here to the ACh receptor sites, quantitatively, at the endplate. The EM autoradiographic technique visualizes, in effect, the distribution of these receptors at the ultrastructural level. We see that the results bear out the expectation that they are located on the postjunctional membrane. While we cannot exclude on the present evidence the alternative interpretation of our histograms, namely that the source of radioactivity is in the cleft substance, this would be contrary to all information on the receptor properties in such

synapses, which are only understandable if the ACh receptor is on the surface of, or embedded in, the membrane. Moreover, electron-microscopic examinations reported by Betz and Sakmann (1971) also favor the postjunctional location of receptors. They found that treatment of muscle with proteolytic enzymes separates the nerve terminals and the Schwann cell coverings from the muscle fibers and removes the cleft substance, to leave only the bare junctional folds. The fibers can then still be depolarized by acetylcholine to about the same extent as before the enzyme treatment, i.e. the receptors effectively remain. In fact, in recent unpublished observations, we have found that ^{3}H-α-BuTX-labeled endplates, after such proteolytic modification, remain labeled in the same sites, which must be in the postsynaptic membrane.

Furthermore, it must be recalled that the axonal membrane mostly does not run parallel to the postjunctional membrane and may be separated from it at areas of folding in these endplates by as much as 5,000 Å (Padykula & Gauthier, 1970). Therefore, the essentially uniform distribution that is found (Fig. 4) only when the junctional fold zone is considered, provides evidence that the distribution of ACh receptors along the postsynaptic membrane does not differ much, if at all, between the mouths and depths of the folds. If the receptors were, for example, only along the membrane in the primary cleft and never in the folds, then the distribution in Fig. 3 would be as narrow as that in Fig. 2, and the wide spread of density through the fold zone seen in Fig. 4 would not be obtained. Similarly, the receptors cannot be confined only to the innermost reaches of the folds.

Other estimations have recently been reported from several laboratories of the density of cholinergic receptor sites at synaptic membranes, based upon diverse methods (Table 3). As can be seen, these studies vary considerably, both in the values obtained and the assumptions used when bulk measurements of receptor labeling in a tissue are converted to a surface density on the synaptic membranes. Only studies 3, 4 and 5 of Table 3 are readily comparable, in that they each employed a direct determination of the density of radioactivity along the synaptic membrane, without requiring an estimate of the surface area of the entire postsynaptic membrane or a basic assumption as to the nature of the particles seen. In study 4 (Barnard *et al.*, 1971*b*) this density determination (which then gave a value of $12{,}000/\mu^2$) was not made directly for the receptor sites, but the latter were measured relative to an internal standard of known synaptic surface density (discussed above), i.e. the ^{3}H-DFP-labeled sites in the endplates. The exact value derived from that study for the mean receptor site density will depend, therefore, upon the value that is taken for the ^{3}H-DFP site density (*see*

Table 3. Reported densities of ACh receptor active sites at postsynaptic membranes (PSM)

Study	Authors	Location of synapse	Sites/μ^2 PSM	Method of labeling	Determination of density
1	Miledi *et al.* (1971)	*Torpedo* electroplaque	10,000	^{131}I-α-BuTX	Total uptake per gram of tissue; total flat ventral surface estimated
2	Karlin *et al.* (1971)	*Electrophorus* electroplaque	3,400	^{3}H-MBTA (Maleimide affinity reagent)	Total uptake per gram of tissue; total subsynaptic surface estimated
3	Bourgeois *et al.* (1972)	*Electrophorus* electroplaque	33,000	^{3}H-Cobra-toxin	EM autoradiography [a]
4	Barnard *et al.* (1971*b*)	Mouse diaphragm; sternomastoid	8,600 [b] 8,800 [b]	^{3}H-α-BuTX	Light microscope autoradiography and comparison with known density of ^{3}H-DFP sites [a]
5	This work	Mouse diaphragm	8,200	^{3}H-α-BuTX	EM autoradiography [a]
6	Miledi & Potter (1971)	Frog sartorius	20,000–100,000	^{131}I-α-BuTX	Total uptake per muscle; estimate of endplate size and assumption of stereology and of 0 to 80% of receptors as being extra-junctional
7	Fambrough & Hartzell (1972)	Rat diaphragm	13,000	^{122}I-α-BuTX	Total uptake in muscle segments; assumption of endplate size and stereology
8	Cartaud *et al.* (1973)	*Torpedo* electroplaque	12,000–15,000	none	Direct count of particles believed to be receptors in membrane by high resolution EM [a]
9	Rosenbluth (1972)	Earthworm body wall	5,000	none	Direct count of granules in membrane believed to be receptors by high resolution EM [a]

[a] This method of density determination does not depend upon an estimate of the total subsynaptic surface for the entire junction.

[b] Previously based upon the standard for ^{3}H-DFP-reactive sites of 12,000/μ^2 (Salpeter, 1969), but now based upon the re-calibrated values of Salpeter *et al.* (1972) for the ^{3}H-DFP sites in these two muscles.

Table 1), and for the most recent determination of the latter (Salpeter *et al.*, 1972) the value provided by study 4 will now be about 8,600 receptor active sites per μ^2 of diaphragm postsynaptic membrane. The three studies cited also have the advantage of analysis at the level of the junctions individually, so that inhomogeneity in the tissue or irregular binding of the labeled reagent outside the synapses does not affect them. In studies 4 and 5, we see that the present EM method and the previous light microscope comparative method give results in complete agreement. This confirms independently the value of 1.0 determined for the ChE-like/receptor site ratio, determined in both studies by other methods.

The other value obtained by EM analysis, that of Bourgeois, Ryter, Menez, Fromageot, Boquet and Changeux (1972), appears to give a significantly larger value, but this is for a different type of tissue, the electric organ. Although the involved stereology of the latter (Bourgeois *et al.*, 1972) complicates the analysis, it may be that there is a real biological difference between the receptor density at the motor endplate and that at the electroplaque postsynaptic membranes. On the other hand, a recent study of the latter membrane using negative staining and high resolution electron-microscopy (*see* study 8, Table 3) shows that particles, interpreted as the ACh receptors in that membrane (since they were seen also in a purified soluble receptor preparation), occur at a density of 12,000 to 15,000/μ^2. This density is reasonably close to our present values for the motor endplate postjunctional membrane. A somewhat similar investigation (*see* study 9, Table 3) reports a density of 5,000 per μ^2 of postsynaptic membrane for stained particles (70 Å diameter) seen in the body wall muscle junction of the earthworm. However, neither of these latter two studies, while highly suggestive, show with certainty that the directly observed membrane particles do represent ACh receptors or that each has one active center.

In a preliminary study (Porter *et al.*, 1973), we reported the receptor density as about 12,000 sites/μ^2 of postjunctional membrane. That result was based upon a less detailed study involving measurements of considerably fewer grains and endplate profiles; moreover, while that report was in press, the paper by Salpeter and Szabo (1972) appeared describing the dose dependence of the L-4 emulsion sensitivity. The latter phenomenon was taken into account in designing the present experiments. For all of these reasons, the present analysis used here involving a much larger number of endplate samples has resulted, we believe, in a statistically more accurate value which should supersede the former, although it is still of the same order.

It is interesting to note that the receptor membrane densities presented here can be used to deduce certain morphometric values which may be

Table 4. Total areas of synaptic membrane at mouse endplate types

Parameter	Fiber type	
	Diaphragm (red)	Sternomastoid (white)
Receptors at whole endplate (A)	2.0×10^7 [a]	8.7×10^7 [b]
Receptors per μ^2 PSM(B)	8,500 [c]	
Area (μ^2) of PSM per endplate (Ratio A/B)	2,300	10,000
Ratio of PSM to AM areas	1:4.5	1:6 [d]
Area (μ^2) of AM per endplate	510	1,650

PSM, postsynaptic membrane; AM, axonal membrane.
[a] From Porter *et al.* (1973). Note that the value depends upon the fiber diameter, and hence, often, the size of the animals. This value refers to the same strain and body size of mice as were used here.
[b] From Barnard *et al.* (1971*a*).
[c] We take this as the best general estimate of mean PSM density of receptors by averaging the values determined here for receptor density (8,200) and by Salpeter *et al.* (1972) for DFP-reactive site density, (8,600 and 8,800) in view of the data of Table 2.
[d] From Salpeter *et al.* (1972).

useful in other studies (Table 4). The total postjunctional membrane per endplate was found by dividing the known values for the total receptors per endplate (Barnard *et al.*, 1971*b*) by the receptor density. The total axonal membrane was determined by using, in addition, the ratio of postjunctional to axonal membranes measured here for mouse diaphragm red fibers or for fibers of the mouse sternomastoid given by Salpeter *et al.* (1972) The fourfold difference in postjunctional membrane for red and white fiber endplates (Table 4) is not unexpected, in the light of the known structural differences between these two fibers. Thus, the endplates of white fibers of the mouse display a marked increase over red fibers in the number of folds, as well as in the depth of each fold (Duchen, 1971). Padykula and Gauthier (1970) report similar structural differences between red and white fiber endplates in the rat, and also describe a longer axon terminal in the white fiber endplate. This latter agrees with the threefold increase in axonal membrane in synaptic contact with the junctional folds for that fiber (Table 4). The 1:4.5 ratio of postjunctional-to-axonal membranes, found in this study and used in deriving the total axonal membrane area, is identical to the morphometric value of Anderssen-Cedergren (1959) for the increase of the postjunctional membrane muscle surface through folding at the mouse red fiber endplate. Salpeter *et al.* (1972) also noted morphometrically a ratio of about 1:5 for the same endplate. The number of α-BuTX-binding

and DFP-reactive sites per endplate increases linearly with the mean fiber diameter.[2] The known numbers of such sites in different fiber types reported previously from this laboratory (Barnard *et al.*, 1971 *a, b*; Porter *et al.*, 1973; *see also* footnote 2) can readily be used, assuming that the mean value of 8,500 sites/μ^2 (Table 4) is universal, to derive in a precisely similar way the postsynaptic membrane areas for a variety of animal and muscle types. Such determinations of synaptic area can, however, only be made for muscle fiber sizes similar to those used in the studies noted. In particular, young and older animals differ in the fiber diameter for the same muscle type, so that this variable must be controlled. The regression of endplate DFP-reactive site content upon fiber diameter given by Wieckowski and Barnard (*see* footnote 2) can be used for interpolation for this purpose.

From autoradiographic evidence at the light microscope level (Barnard *et al.*, 1971 *b*) and also from data from liquid scintillation counting of extracts of muscle-bound ^{3}H-α-BuTX (Porter *et al.*, 1973), it has been found that the number of AChE plus related DFP-reactive sites at the motor endplate is (in various species) equal to the number of ACh receptor sites there. This suggested an equality of their densities on the postsynaptic membrane. A proof of this hypothesis is provided by the direct density measurements made here. This reinforces the suggestion made of some spatial relationship between the two types of molecules at the endplates, although it is known that they are distinct and separable entities (Barnard *et al.*, 1971 *b*; Betz & Sakmann, 1971; Hall & Kelly, 1971). The density of 8,000 to 9,000 sites per μ^2 of postsynaptic membrane that has been measured here at the mouse diaphragm muscle endplate (for both the receptor and the ^{3}H-DFP sites) has been found also at the mouse sternomastoid muscle endplate (for the ^{3}H-DFP-reactive sites) by Salpeter (1969) and Salpeter *et al.* (1972). In fact, the 1:1 relationship between these two types of sites has been shown, at the whole endplate level, to hold for endplates in a variety of vertebrate muscles (Barnard *et al.*, 1971 *b*). It can be speculated that there is a constant density of packing in the membrane which is characteristic of the ACh receptor molecules at all motor endplates.

This population of about 8,500 subunits of ACh receptor per μ^2 (taken as structures each carrying one active center of the receptor) would occupy a rather high fraction of the membrane surface, as was noted by Barnard *et al.* (1971 *b*). In fact, this would be about 20% of the area available to close-packed spherical molecules of their size. This value is based upon

2 Wieckowski, J., Barnard, E. A. 1974 Cholinesterases and related molecules at individual neuromuscular junctions. II. The numbers of their active centers in various muscle types. *Mol. Pharmacol. (In press)*

a molecular weight of about 50,000, deduced (Karlin, Prives, Deal & Winnik, 1971; Meunier, Olsen, Menez, Fromageot, Boquet & Changeux, 1972) for the subunit of electroplax ACh receptor, and upon the assumption that it is a regular globular protein (corrected partial specific volume = 0.73: Meunier *et al.*, 1972; *cf.* Bourgeois *et al.*, 1972). However, the molecular weight of the muscle endplate receptor subunit has not yet been established. Cholinesterase-type units would occupy an additional equal area if in the membrane, but they need not actually be in it and may lie just above it (Barnard, 1974).

Note Added in Proof. While this paper was in press, an article [M. M. Salpeter and M. E. Eldefrawi, *J. Histochem. Cytochem.* **21**:796 (1973)] was published which also estimates the surface area of the postsynaptic membrane at endplate types such as those considered here. These estimates were made using the values of Salpeter *et al.* (1972) for the densities of DFP-reactive sites at that membrane, divided into the known total number of DFP-reactive sites provided by Rogers *et al.* (1969) and Barnard *et al.* (1971*b*). These surface area values agree well with ours, as expected in view of the agreement already noted of the DFP-reactive site density with our receptor active center density. Values are given by Salpeter and Eldefrawi for receptor active center density, but these are deduced values, being based upon (a) the total numbers of receptors as determine by Barnard *et al.* (1971*a*) or (on the basis of scintillation counting data on labeled muscle and a simplified model for the shape of an end-plate) by Fambrough and Hartzell (1972), and (b) the calculated postsynaptic areas. Our values, on the other hand, [and also those reported earlier (Porter *et al.*, 1973)] represent a direct determination of both receptor density and location.

This work was supported by Grant No. GM-11754 of the U.S. National Institutes of Health. During this study, C.W.P. was supported by Training Grant No. 01500 from the National Institute of General Medical Sciences. We are grateful to Dr. G. Colin Budd (Medical College of Ohio at Toledo) for his instruction and advice on quantitation in EM autoradiography and for kindly calibrating the sensitivity of our emulsion.

References

Albuquerque, E. X., Barnard, E. A., Chiu, T. H., Lapa, A., Dolly, J. O., Jaenssen, S. E., Daly, J., Witkop, B. 1973. Ionic conductance modulator and acetylcholine receptor sites in the mouse neuromuscular junction: Evidence from specific toxin reactions. *Proc. Nat. Acad. Sci.* **70**:949

Anderssen-Cedergren, E. 1959. Ultrastructure of motor endplate and sarcoplasmic components of mouse skeletal muscle fiber. *J. Ultrastruct. Res.* (Suppl.) **1**:1

Barnard, E. A. 1970. Location and measurement of enzymes in single cells by isotopic methods. *Int. Rev. Cytol.* **29**:213

Barnard, E. A. 1974. Enzymic destruction of acetylcholine. *In:* The Peripheral Nervous System. J. I. Hubbard, editor. Plenum Press, New York. *(In press)*

Barnard, E. A., Rymaszewska, T., Wieckowski, J. 1971*a*. Cholinesterases at individual neuromuscular junctions. *In:* Cholinergic Ligand Interactions. D. J. Triggle, J. F. Moran and E. A. Barnard, editors. p. 175. Academic Press Inc., New York

Barnard, E. A., Wieckowski, J., Chiu, T. H. 1971*b*. Cholinergic receptor molecules and cholinesterase molecules at mouse skeletal muscle junctions. *Nature* **234**:207

Betz, W., Sakmann, B. 1971. "Disjunction" of frog neuromuscular synapses by treatment with proteolytic enzymes. *Nature, New Biol.* **232**:94

Bourgeois, J.-P., Ryter, A., Menez, A., Fromageot, P., Boquet, P., Changeux, J.-P. 1972. Localization of the cholinergic receptor protein in *Electrophorus* electroplax by high resolution autoradiography. *FEBS* **25**:127

Budd, G. C. 1971. Recent developments in light and electron microscope radioautography. *Int. Rev. Cytol.* **31**:21

Cartaud, J., Beneditt, E. L., Cohen, J. B., Meunier, J.-C., Changeux, J.-P. 1973. Presence of a lattice structure in membrane fragments rich in nicotinic receptor protein from electric organ of *Torpedo marmorata*. *FEBS* **33**:109

Duchen, L. W. 1971. An electron microscopic comparison of motor-endplates of slow and fast skeletal muscle fibres of the mouse. *J. Neurol. Sci.* **14**:37

Fambrough, D. M., Hartzell, H. C. 1972. Acetylcholine receptors: Number and distribution at neuromuscular junctions in rat diaphragm. *Science* **176**:189

Gauthier, G. F., Padykula, H. A. 1966. Cytological studies of fiber types in skeletal muscle. A comparative study of the mammalian diaphragm. *J. Cell Biol.* **28**:333

Hall, Z. W., Kelly, R. B. 1971. Enzymatic detachment of endplate acetylcholinesterase from muscle. *Nature, New Biol.* **232**:62

Karlin, A., Prives, J., Deal, W., Winnik, M. 1971. Affinity labeling of the acetylcholine receptor in the electroplax. *J. Mol. Biol.* **61**:175

Meunier, J. C., Olsen, R. W., Menez, A., Fromageot, P., Boquet, P., Changeux, J.-P. 1972. Some physical properties of the cholinergic receptor protein from *Electrophorus electricus* revealed by a tritiated α-toxin from *Naja nigricollis* venom. *Biochemistry* **11**:1200

Miledi, R., Molinoff, P., Potter, L. T. 1971. Isolation of the cholinergic receptor protein of *Torpedo* electric tissue. *Nature* **229**:554

Miledi, R., Potter, L. T. 1971. Acetylcholine receptors in muscle fibres. *Nature* **233**:599

Padykula, H. A., Gauthier, G. F. 1970. The ultrastructure of the neuromuscular junctions of mammalian red, white and intermediate skeletal muscle fibers. *J. Cell Biol.* **46**:27

Porter, C. W., Chiu, T. H., Wieckowski, J., Barnard, E. A. 1973. Types and locations of cholinergic receptor-like molecules in muscle fibres. *Nature, New Biol.* **241**:3

Rogers, A. W., Darzynkiewicz, Z., Barnard, E. A., Salpeter, M. M. 1966. Number and location of acetylcholinesterase molecules at motor endplates of the mouse. *Nature* **210**:1003

Rogers, A. W., Darzynkiewicz, Z., Salpeter, M. M., Ostrowski, K., Barnard, E. A. 1969. Quantitative studies on enzymes in structures in striated muscles by labeled inhibitor methods. I. The number of acetylcholinesterase molecules and of other DFP-reactive sites at motor endplates measured by radioautography. *J. Cell Biol.* **41**:665

Rosenbluth, J. 1972. Myoneural junctions of two ultrastructurally distinct types in earthworm body wall muscle. *J. Cell Biol.* **54**:566

Salpeter, M. M. 1967. Electron microscope radioautography as a quantitative tool in enzyme cytochemistry. I. The distribution of acetylcholinesterase at motor endplates of a vertebrate twitch muscle. *J. Cell Biol.* **32**:379

Salpeter, M. M. 1969. Electron microscope radioautography as a quantitative tool in enzyme cytochemistry. II. The distribution of DFP-reactive sites at motor endplates of a vertebrate twitch muscle. *J. Cell Biol.* **42**:122

Salpeter, M. M., Bachmann, L. 1964. Autoradiography with the electron microscope. A procedure for improving resolution sensitivity and contrast. *J. Cell Biol.* **22**:469

Salpeter, M. M., Bachmann, L., Salpeter, E. E. 1969. Resolution in electron microscope radioautography. *J. Cell Biol.* **41**:1

Salpeter, M. M., Plattner, H., Rogers, A. W. 1972. Quantitative assay of esterases in endplates of mouse diaphragm by electron microscope autoradiography. *J. Histochem. Cytochem.* **20**:1059

Salpeter, M. M., Szabo, M. 1972. Sensitivity in electron microscope autoradiography. I. Effect of radiation dose. *J. Histochem. Cytochem.* **20**:425

Wilson, I. B., Ginsburg, S., Quan, C. 1958. Molecular complementariness as a basis for reactivation of alkyl phosphate inhibited enzyme. *Arch. Biochem. Biophys.* **77**:286